Remote Sensing of Environment 220 (2019) 41–50

Contents lists available at ScienceDirect

Remote Sensing of Environment

journal homepage: www.elsevier.com/locate/rse

Satellite remote sensing of canopy-forming kelp on a complex coastline: A novel procedure using the Landsat image archive

Wiebe Nijland[a,b,c,*], Luba Reshitnyk[a], Emily Rubidge[d,e]

[a] Hakai Institute, Calvert Island, British Columbia, Canada
[b] School of Environmental Studies, University of Victoria, Victoria, BC, Canada
[c] Department of Physical Geography, Utrecht University, Utrecht, the Netherlands
[d] Institute of Ocean Sciences, Fisheries and Oceans Canada, Sidney, BC, Canada
[e] Department of Forest and Conservation Sciences, University of British Columbia, Vancouver, BC, Canada

ARTICLE INFO

Keywords:
Landsat
Worldview 2
Canada
Pacific
Google earth engine
Kelp
Macrocystis pyrifera
Nereocystis luetkeana

ABSTRACT

Kelp forests are highly productive and diverse coastal marine ecosystems which have high variability in extent and biomass spatially and through time. Mapping and monitoring their distribution is integral to understanding the ecology of kelp forests and to inform marine protected area planning. Canada's Pacific coast presents specific challenges to mapping canopy forming kelp with thousands of kilometers of coastline, complex topography, and a large tidal range. While in situ methods and manual interpretation of aerial photography are commonly used to map canopy-forming kelp at local or regional scales, these methods are prohibitively expensive for continued large-area application. Historical and current available inventories of kelp extent are therefore incomplete for Canada's Pacific Coast. The advent of Google Earth Engine, a cloud-computing platform with a repository of Landsat imagery, provides an opportunity to apply Landsat image archive analyses and integrate temporal compositing and filtering to obtain unprecedented data on historical and current kelp extents. However, the effects of the spatial resolution and temporal coverage for mapping canopy-forming kelp in regions with complex coastlines and large tidal ranges are unknown. The objectives of this study were twofold: (1) develop a tool within Google Earth Engine to automate the detection of kelp using the Landsat satellite image archive, and (2) quantify the associated limitations for mapping the surface extent of canopy-forming kelp by comparing Landsat derived kelp extent with extents derived from WorldView-2 satellite imagery. The results indicate that the overall accuracy of the developed method is high at 80% and very close in accuracy to WorldView-2 data, but no detection is feasible within approximately one 30 m pixel from the shoreline. The interaction between the spatial resolution, kelp bed size, and bed configuration affected the detected kelp extent, as did the tide level during image acquisition. For both sensors, a 2 m increase in tide resulted in a 40% decrease in kelp extent detected. The Google Earth Engine kelp mapping tool presented provides an efficient and transferable method for mapping canopy kelp extent, and the only currently available method to reconstruct coast wide kelp development for the past three decades. The presented tool has applications in conservation and management planning, for example in creating a baseline of past kelp extent and examining trends in kelp forest variability.

1. Introduction

Kelp species are globally distributed in cold and temperate waters (Raffaelli and Hawkins, 1996) and hold a vital position in nearshore environments and ecosystems. Kelp are a morphologically diverse clade of large canopy-forming marine macroalgae (order: *Laminariales*) that form dense communities –kelp forests– along rocky coastlines. Kelp ecosystems are biodiversity hotspots, providing essential habitat for juvenile and adult marine organisms (Dayton, 1985; Steneck et al., 2002), and primary producers in the near-shore environment who provide energy and nutrients for both marine (Duarte and Cebrian, 1996; Harrold et al., 1998; Krumhansl and Scheibling, 2012) and terrestrial food webs (Lastra et al., 2008; Orr et al., 2008; Polis and Hurd, 1996). Macro algae represent important commercial value worldwide; on the Canadian Pacific coast kelp species are harvested on larger scales both commercially and by local First Nations for herring spawn on kelp harvest.

Kelp ecosystems are easily perturbed (Krumhansl et al., 2016; Steneck et al., 2002), with reductions in kelp abundance having direct consequences for coastal biodiversity (Marzinelli et al., 2015; Steneck et al., 2002) and productivity (Clasen and Shurin, 2015; Wilmers et al., 2012).

* Corresponding author at: Department of Physical Geography, Utrecht University, Utrecht, the Netherlands.
E-mail address: geo.uu@wiebenijland.nl (W. Nijland).

https://doi.org/10.1016/j.rse.2018.10.032
Received 3 May 2018; Received in revised form 25 September 2018; Accepted 22 October 2018
Available online 27 October 2018

Inventories of the extent and biomass of canopy-forming kelps are therefore important to understand the health and state of nearshore ecosystems. A comprehensive kelp inventory and map is also crucial for sustainable harvest management, marine protected area planning, and ecological research. For example, as part of Canadian national and provincial guidance on the development of Marine Protected Area (MPA) networks, a key design principle is the inclusion of representative habitats within the planning region in the resulting MPA network (Government of Canada, 2011; Canada-British Columbia, 2014). A comprehensive map of kelp forests, a priority habitat for the planning process (DFO, 2017), even at a broad scale, would fill an important data gap in the MPA network planning process in British Columbia (BC).

In BC, studies and inventories of kelp extent and biomass to date have been based on the interpretation of aerial photographs paired with in situ measurements. However, these inventories have been both spatially and temporally discontinuous with the last inventory conducted in 2006 (Sutherland et al., 2008), and previous to that in 1993 (Field, 1996), presenting an immediate demand for more current information on the kelp distribution in BC. Furthermore, these surveys only covered a section of the Central Coast, which makes up only a fraction of the approximately 25,000 km of shoreline in the province. Where more regular time series are available, they are based on repeated surveys of permanent field quadrats which provide high quality information including species inventory and biomass, but have a limited spatial coverage (Krumhansl et al., 2016; Watson and Estes, 2011). These temporal studies indicate high levels of variability in kelp cover (Shaffer, 2000; Watson and Estes, 2011) which questions the value of widely spaced snapshots for trend analysis. Trends in kelp abundance in the Gulf of Alaska and on the BC coast have been linked to the reintroduction of sea otters (*Enhydra lutris*) and their predation of urchins who feed on kelps (Dean et al., 1984; Estes and Duggins, 2010; Markel and Shurin, 2015; Watson and Estes, 2011). As mentioned, there is no current or complete inventory of canopy-forming kelp for BC and no method providing a rapid assessment of kelp coastwide. Mapping the distribution and quantity of kelp and monitoring the quality of kelp habitats are key priorities for multiple marine spatial planning initiatives including the identification of Ecologically and Biologically Significant Areas (EBSAs) (, DFO, 2018), marine protected area network design (Canada-British Columbia, 2014), and oil spill sensitivity and response planning (Hannah et al., 2017).

Mapping kelp using traditional techniques, either through the collection of field data or visual interpretations aerial imagery, is prohibitively expensive to cover large geographical regions such as the over 25,000 km long coastline present in BC. The advent of satellite remote sensing has provided new, more efficient methods for mapping kelp extent and biomass. Kelps have spectral characteristics similar to those of terrestrial plants, with high reflectance in the near-infrared portion of the electromagnetic spectrum which strongly contrast with water (Cavanaugh et al., 2010). Therefore, satellite imagery from most common sensor platforms provides the necessary information to derive surface kelp extent. However, detection is limited to kelp present near the water surface due to the strong attenuation of the infrared signal by water.

Much of the work on satellite detection of kelps has focused on giant kelp (*Macrocystis pyrifera*) in California (e.g. Bell et al., 2015a; Bell et al., 2015b; Cavanaugh et al., 2011). Adapting these methods to coastal British Columbia represents a unique challenge. Firstly, a more topographically complex coastline of thousands of islands, inlets, and fjords means more complex habitat for kelp. Canopy-forming kelp beds in British Columbia are characterized by smaller beds often occurring as strips fringing the shore compared to the continuous forests in California of multiple of kilometers long. Secondly, two dominant canopy-forming kelp species occur on the Central Coast of British Columbia – giant kelp (*Macrocystis pyrifera* L.), and bull kelp (*Nereocystis luetkeana* Mertens.) – which are different in both their physical structure and phenology. Giant kelp is a perennial species, with each plant consisting of multiple fronds with blades along the entire length of each frond. Bull kelp is an annual species with a single smooth stipe ending in a bulb with multiple blades.

High resolution commercial satellite imagery (< 5 m resolution) provides the capacity to map terrestrial and marine regions with high spatial detail. This detail is especially relevant in irregularly shaped or patchy kelp beds and in narrow kelp beds that fringe steeper shore zones. The WorldView-2 satellite provide high spatial resolution imagery (2 m) and high spectral resolution (8 bands). While additional spectral resolution has been shown to improve species level mapping (Botha et al., 2013), it is unlikely to be able to differentiate between two species of brown algae due to similarities in the pigmentation. The sensor's finer resolution permits the detection of smaller beds, which are often closer to shore. However, most imagery from high resolution sensors (e.g. WorldView-2) is provided as a commercial service and therefore must be tasked to cover regions of interest.

The Landsat series of sensors have been collecting near global coverage of multispectral satellite imagery at a 30 m spatial resolution since 1984 (https://landsat.gsfc.nasa.gov/) with Landsat 8 (LS8), launched in 2013, as the most recent operational sensor in the series. The continuous image collection and free availability to the public since 2008 makes the Landsat series the most commonly applied image source for terrestrial mapping (Banskota et al., 2014; Cohen and Goward, 2004); and, to a lesser extent, freshwater (Lin et al., 2018) and marine habitat mapping (Hossain et al., 2016; El-Askary et al., 2014; Torres-Pulliza et al., 2013). Launched in 2009, Google Earth Engine has an online repository of Landsat imagery, as well as imagery from other satellite sensors, creating a platform for researchers to analyze data and bypass downloading hundreds of individual scenes. Google Earth Engine exposes remotely sensed imagery datasets (including Landsat) to direct analysis by the community and provides an online platform to access computing resources to process and disseminate geospatial results (Gorelick et al., 2017) and removes the requirement of downloading hundreds to thousands of individual images for processing and analysis. The GEE platform has been rapidly adopted by researchers and resource managers for many applications including landcover-landuse change in terrestrial environments (Zurqani et al., 2018; Murray et al., 2018), freshwater algal blooms (Lin et al., 2018), and in the marine environment to monitor seagrasses (Traganos et al., 2018). Applications for marine macroalgae, specifically canopy-forming kelps, are thus far not available.

The availability of the Landsat image archive within Google Earth Engine presents the opportunity to analyze kelp time series since 1984 and detect the persistence of kelp cover and trends. Previous work by Cavanaugh et al. (2011) developed methods for mapping giant kelp (*Macrocystis pyrifera*) extent and biomass within the Santa Barbara Channel, California using Landsat 5 TM imagery. However, these methods rely on downloading and processing individual image. Additional, manual delineation of kelp classified pixels is necessary to correctly designate pixels that are erroneously classified as kelp due to clouds, haze and data gaps. The Santa Barbara channel represents very different study from the Central Coast of British Columbia with regards to coastline complexity, tidal regimes and weather. With more frequent and persistent cloud cover, and generally smaller kelp beds compared to California, mapping kelp extent in BC requires methods that remove the need for user selection of individual image scenes and manual delineation of kelp beds.

This paper presents a novel procedure for automated mapping of canopy forming kelp extent at the water surface using temporal compositing of Landsat images from 1984 to 2016. We examine the abilities and limitations of mapping kelp canopies using the Landsat archive by comparing the results to WorldView-2 derived kelp extents and field plots on the Central Coast region of British Columbia, Canada. The objectives of this paper are to present the new Landsat procedure, to evaluate its accuracy to detect canopy-forming kelps, and to analyze the spatial and temporal characteristics of the results. Specifically we compare kelp extent derived from Landsat archive images and co-located high resolution satellite imagery (WorldView-2) to examine (1) the accuracy of detecting canopy-forming kelp compared to field plots, (2) the effects of image resolution on the detection of kelp extent, (3) differences in the response of kelp detection between areas with differing characteristics in near-shore

morphology, kelp distribution, and patch sizes and (4) the effect of tide on detecting kelp extent. Using the newly developed mapping tool, we present a first look at changes in kelp cover on the Central Coast of British Columbia region during the last three decades.

2. Methods

2.1. Study region

The Central Coast of British Columbia comprises a region ranging from 51.16–52.25° latitude. This region is a part of the Queen Charlotte Sound marine ecosection and falls within two oceanographic subregions including Mainland Fjords and Eastern Queen Charlotte Sound (BCMCA: 2011 - http://bcmca.ca/maps-data/atlas/). The oceanic conditions of this region are seasonally influenced with sea surface temperatures coldest in March (7 to 8 °C) and warmest in August (13 to 15 °C) (Jackson et al., 2015). Tides in the region range from 3 to 5 m and are semidiurnal (Thomson, 1981). Northwesterly winds common from May to September create a weak upwelling-dominated season while southeasterly winds from October to April create a downwelling-dominated season. Currents within Queen Charlotte Sound are largely wind-driven (Crawford et al., 1985). Over the past 40 years, an increase in cumulative upwelling and downwelling has been observed on British Columbia's north coast (Foreman et al., 2011).

The region is topographically complex with thousands of kilometers of coastline including over 1500 islands and multiple glacially mediated fjords. Shorelines are a varied combination of rocky headlands and mixed sedimentary beaches. Nearshore areas are influenced by many physical factors (e.g. waves, tidal currents, temperature, salinity, light penetration) which, in turn influence nearshore floral communities of algae and seagrass. The Central Coast region presents a high algal diversity along its shallow (< 20 m) rocky habitats. Canopy-forming kelp beds are predominantly composed of bull kelp (*Nereocystis luetkeana*) and giant kelp (*Macrocystis pyrifera*). Other canopy forming kelp (e.g. *Egresia menziesii*) are present in the region in much lower abundances.

Sea otters, extirpated from British Columbia in 1929 and reintroduced in the late 1960's and early 1970's are relatively abundant along the Central Coast (Nichol et al., 2015). Sea otters are well documented in their role of shaping kelp forest ecosystems (Estes and Duggins, 2010; Estes and Palmisano, 1974) and populations along the Central Coast are currently increasing (Nichol et al., 2015). The region is the present and ancestral home of several First Nation communities,

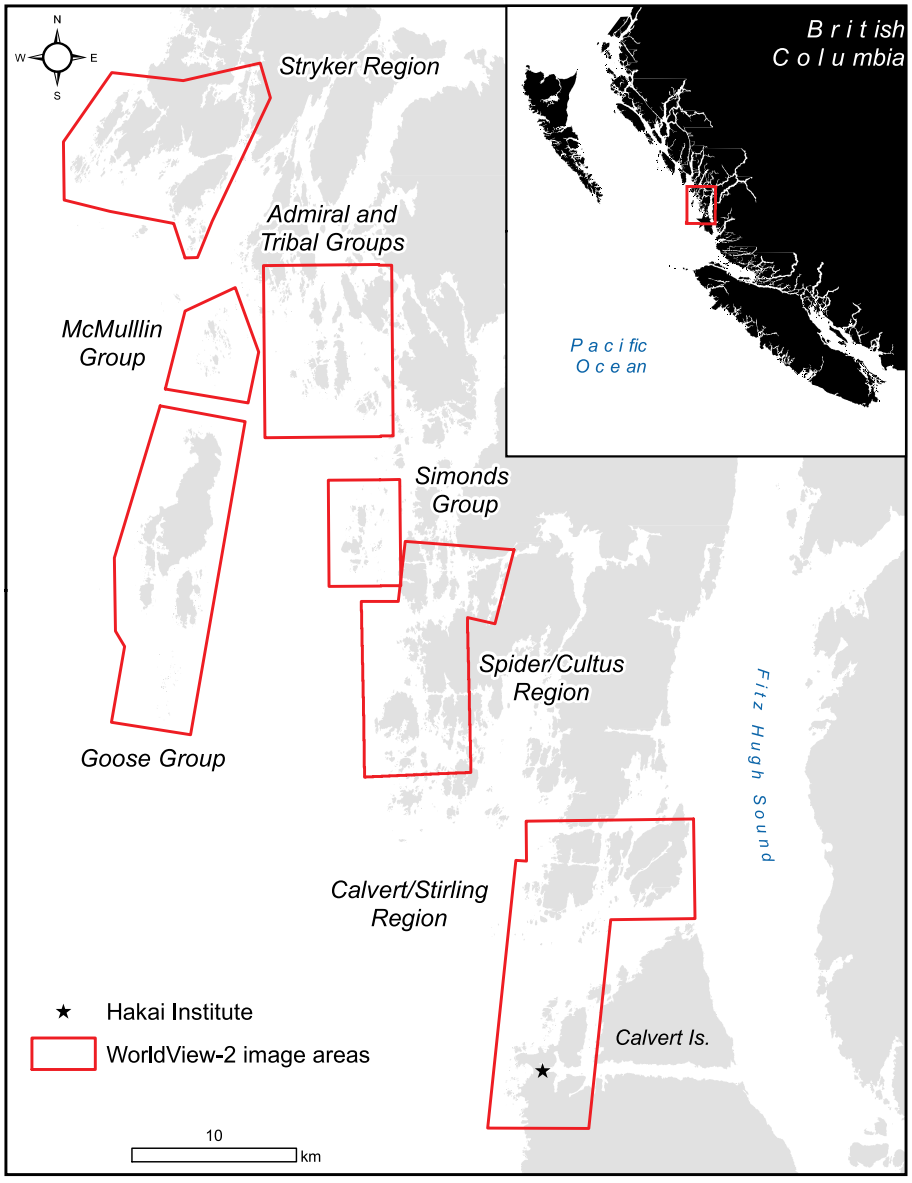

Fig. 1. Study area showing the extent of WorldView-2 imagery used in this study.

Table 1
Images used for tide stage comparison from Landsat 8 and WorldView-2 sensors for the McMullin region.

Sensor	Acquisition date	Tide level [m above chart datum]
Landsat 8 (tile 052024)	2014, August 17th	1.5
Landsat 8 (tile 051024)*	2014, August 10th	3.6
WorldView-2	2014, August 13th	2.7
WorldView-2*	2014, July 17th	0.6

* Imagery from this date was used to examine the effects of tidal state on kelp detection (McMullin region subset).

which have lived on the coast for thousands of years (McLaren et al., 2015). These communities continue to harvest local marine resources including shellfish, fish and algae species. Commercial activity in the region is largely dominated by fishing and logging industries.

In this study, we focused on the region from Stryker Island in the north to Calvert Island in the south which is the focal study area of the Hakai Institute (Fig. 1). The Hakai Institute is a scientific research institution conducting long-term research at remote locations on the coastal margin of British Columbia. It has been conducting research on the Central Coast since 2010.

2.2. Satellite image data

Two sources of satellite imagery were used in this study: The Landsat image archive from 1984 to 2016, and Worldview-2 images from 2014 and 2012. The Landsat archive was used within Google Earth Engine to develop a tool to examine kelp extent at decadal time scales. WorldView-2 images were acquired for seven areas of the Central Coast (Fig. 1). For the McMullin Group we use two WorldView-2 images and two single date Landsat 8 OLI scenes from the summer of 2014 to evaluate the effect of tide on the detection of kelp extent (Table 1).

2.2.1. WorldView-2 imagery - processing and kelp classification

Launched in 2009, WorldView-2 is a multispectral sensor has a 17.7 km swath which collects imagery with a 2 m spatial resolution and 8 spectral bands covering coastal, blue, green, yellow, red, red edge, and two near-infrared bands (DigitalGlobe, 2016). WorldView-2 imagery used in this study was collected on August 13th, 2014 for all areas with the exception of Stryker/Athlone (collected July 22nd, 2012). Images were processed to surface reflectance using ATCOR (Richter and Schlapfer, 2012) with mid-latitude summer and maritime aerosol settings and a constant visibility of 100 km. Tide level at the time of image acquisition was 2.7 m (above chart datum). For a small part of the study area (McMullin Group) an additional image was available collected July 17th, 2014 during a 0.6 m tide (Table 1) and was processed following the same methodology.

Each WorldView-2 scene was classified into two classes (water and kelp) using a supervised maximum likelihood classifier using ENVI image processing software (Harris Geospatial Solutions, 2017). A minimum of 100 pixels were selected to for each class based on visual interpretation of the imagery. The kelp class grouped canopy-forming kelp species (*N. luetkeana* and *M. pyrifera*) as a single group. Where necessary, classifications were generated separately for individual image scenes which showed varying radiometric responses. Land area (above the water line) and water deeper than 20 m (below chart datum) were masked using marine chart bathymetry. Masking land and deep water reduced processing times and regions of potential misclassification.

2.2.2. Landsat imagery and pre-processing

The Landsat series of satellite sensors have been collecting near global coverage every 16 days and represents one of the most extensive datasets for surface land mapping. While changes in sensor configuration have changed subtly over time, the sensors record multiple bands including blue, green red and near infrared at a 30 m spatial resolution. Landsat 5 was launched in 1984 and decommissioned in 2013. In 1997, Landsat 7 was launched, however, in 2003, the Landsat 7 ETM + sensor experienced a failure to the line Scan Line Corrector but continues to collect imagery. Landsat 8 was launched in 2013. The entirety of the Landsat collection is available within Google Earth Engine.

For each year, all available scenes with a maximum cloud cover of 80% acquired between June 1st and Sept 30th were selected. This date range was chosen to coincide with annual peak kelp biomass for the region. Clouded and cloud shade pixels were removed using the Fmask labels (Zhu et al., 2015). Because automated atmospheric correction is problematic over large water bodies (Clark et al., 1997; Gerace and Schott, 2012; Hu et al., 2001; Mao et al., 2016), we used top of atmosphere reflectance collections of the Landsat 4-TM, 5-TM, 7-ETM + and 8-OLI sensors (LT4_L1T_TOA_FMASK, LT5_L1T_TOA_FMASK, LE7_L1T_TOA_FMASK, and LC8_L1T_TOA_FMASK).

2.3. Google earth engine kelp mapping tool

We created a time series of annual composites of kelp extent from 1985 to 2016 from the Landsat archive of images using the Google Earth Engine (Gorelick et al., 2017). Land areas were masked based on the Joint Research Centre (JRC) surface water product (Pekel et al., 2016) (JRC/GSW1_0/GlobalSurfaceWater) as areas with a water frequency of < 60%. The 60% cut-off was chosen to include tidal areas as land, but exclude heavily kelp covered areas that may occasionally be labeled as non-water in the JRC product. The land mask was buffered by 30 m (1 pixel) to exclude mixed pixels (land, tidal areas, water and potentially kelp). Initial attempts of classifying kelp identified that including the buffered area severely increased false positive detections of kelp. In British Columbia, fringing kelp beds are commonly present near the shoreline, therefore we examined the consequences of this 30 m buffer in the coastal zone using WorldView-2 imagery to assess the extent of kelp that is missed using the methods we propose for Landsat imagery (see section 2.6).

For each pixel, the normalized difference vegetation index (NDVI) was calculated and classified as water or potential kelp using an NDVI threshold of 0.05. Like terrestrial vegetation, canopy-forming kelp present at the ocean's surface displays a high reflectance of near infrared light and NDVI has been shown to be an effective proxy for mapping kelp extent and abundance (Cavanaugh et al., 2010). The NDVI threshold cut-off was selected based on trial and error in order to capture regions of sparse kelp cover (i.e. low NDVI values) while excluding open water. For each year a maximum NDVI value composite was created discarding any pixels which were classified as potential kelp in < 30% of the available cloud free pixels. For example, for a pixel with 6 cloud free images in a year, the NDVI value must be > 0.05 in two or more image scenes in order to be classified as kelp. For each year, the total extent of kelp is retained as well as a maximum NDVI value composite representing kelp cover density. The procedure achieves the maximum detected kelp extent and density from the image collection while removing ephemeral high NDVI areas caused by marine phenomena such as microalgal blooms or high turbidity (Hu, 2009; Ritchie et al., 2003) or the presence of sun glint which is known to adversely affect remotely sensed imagery over water (Hedley, 2003; Kay et al., 2009). Fig. 2 summarizes the image classification process (Fig. 2).For the period between 1985 and 2016 there were on average 4.8 clear images per pixel per year between June and September (Fig. 3). This number of observations combined with the effects of tides on detectable kelp on the water's surface makes yearly detected areas highly variable and not fully representative of the actual extent of kelp by year. To account for the temporal variability in kelp detection due to differences in tidal heights and detection, we examined trends in kelp extent by aggregating annual kelp outputs over three decades

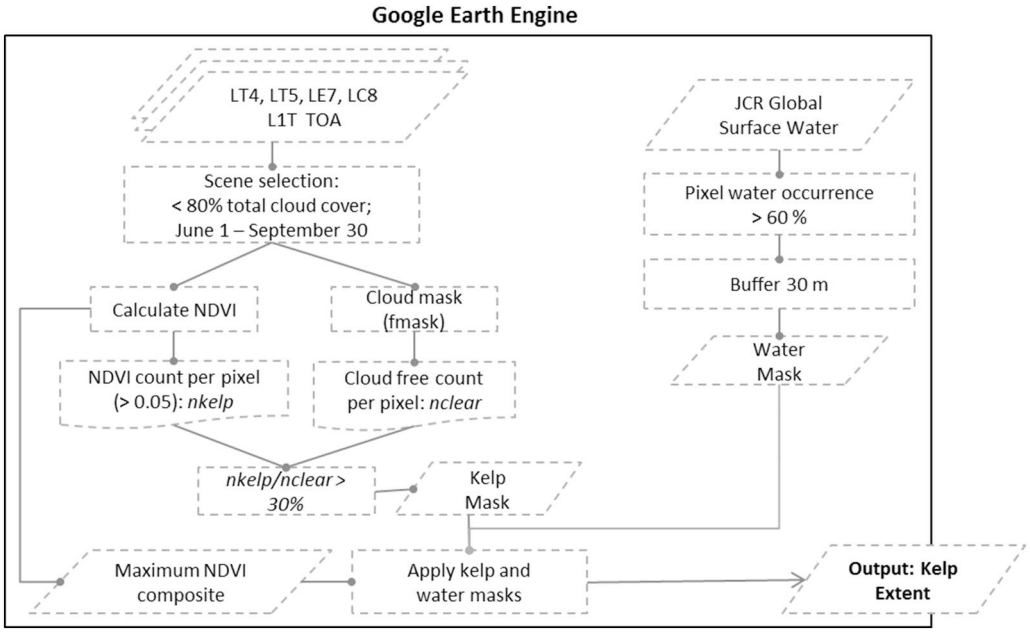

Fig. 2. Flow diagram of the Earth Engine processing algorithm to derive yearly kelp information from the Landsat archive.

(1985–1996, 1997–2006 and 2007–2016), reducing variability and achieving more stable outputs that are better suited for trend analysis.

2.4. Accuracy assessment

Accuracy of both the WorldView-2 and Landsat derived kelp classification was evaluated using field verified plots stratified by landcover (kelp and water). Plot data for kelp were collected from July 9th – 13th, 2014 from a boat. A 2 × 2 m quadrat was used to collect the spatial location, presence, species type, and relative density of kelp. Location coordinates were collected using Topcon GR5 survey grade global positional system, providing < 2 m horizontal accuracy. Of the original field data (n = 210), only points that overlapped with satellite and imagery and a least 30 m apart were kept (n = 134) so that no two field plots occurred within the same Landsat pixel. Because the points were kelp only, we added 100 points representing water. Water points were randomly distributed within the 0–20 m water depth mask and checked to contain only water by visual image interpretation. The point data were used to assess the accuracy of the classification and are considered representative of the Landsat pixel they intersect, for the WorldView-2 kelp detection a 5 m buffer was added to the points, matching any kelp within that radius to account for positional accuracy of the imagery. The field data were not collected in some image regions as these images were purchased after field data collection. Accuracy is evaluated in the form of a confusion matrix (Stehman and Czaplewski, 1998).

2.5. Spatial resolution effects on detected kelp extent

Nearshore bathymetry strongly determines kelp bed structure and size. When nearshore bathymetry varies between regions, this may affect the detectability of surface canopy kelp within an image based on sensors spatial resolution. We compared the extent of kelp detected in the WorldView-2 and Landsat imagery for the island groups and regions present in our dataset (Fig. 1). We considered these image regions to be relatively homogeneous in their nearshore characteristics (e.g. bathymetry, geomorphology). By comparing kelp detection across regions we intended to examine the performance of the detection methods in a range of conditions in which kelp may occur within the study region (e.g. nearshore fringing beds compared to offshore reefs).

To ensure comparable results between sensors, Landsat and WorldView-2 results were clipped to the same area covered by each WorldView-2 scene (Fig. 1). We specifically examined the areal extent of kelp present within 30 m of shore in WorldView-2 imagery (i.e. fringing) to obtain an estimate of how much kelp extent is missed in Landsat imagery with the application of the 30 m buffer to the land mask which is needed to avoid misclassification of mixed pixels as kelp using Landsat imagery.

The spatial resolution of the image sensor will determine the size of kelp bed patches that the sensor will detect (where a patch is considered a contiguous region of surface canopy kelp). To analyze the effect of the kelp patch size on kelp detection by the Landsat procedure we resampled the WorldView-2 derived kelp extents to the same spatial resolution of Landsat imagery (30 m pixels). For each of the resampled WorldView-2 kelp derived extents we calculated the percent cover of kelp from the original 2 m product in order to examine the minimum fraction of surface kelp necessary for classifying a pixel as kelp within the coarser (30 m) resolution imagery. The cover statistics for the resampled WorldView-2 dataset were aggregated for each image region and compared. For each image region we also compared total kelp extent per region with the minimum fraction of kelp (i.e. the minimum threshold of kelp extent needed in order for a 30 m pixel to be classified as kelp). The patterns reflect the effects of using the Landsat resolution pixels in the different island groups in the study area compared to WorldView-2.

2.6. Tide sensitivity

Tidal height affects bed size present at the ocean surface (Britton-Simmons et al., 2008). We examined the effects of tidal state on the detection of surface canopy kelp for both sensors for the McMullin Group region. In this region, WorldView-2 and Landsat 8 images were available for two pairs of dates very close in time (Table 1) (other regions within the imagery were obfuscated by clouds). Each pair of images had a difference in tidal height of 2 m. While our comparison of tidal states was limited to this region due to image availability, the comparison provides relevant information on the sensitivity of detecting kelp on the water surface at different tidal stages.

3. Results

3.1. Accuracy assessment

In reference to field observations of kelp presence-absence, overall accuracy of WorldView-2 was slightly higher than the Landsat product

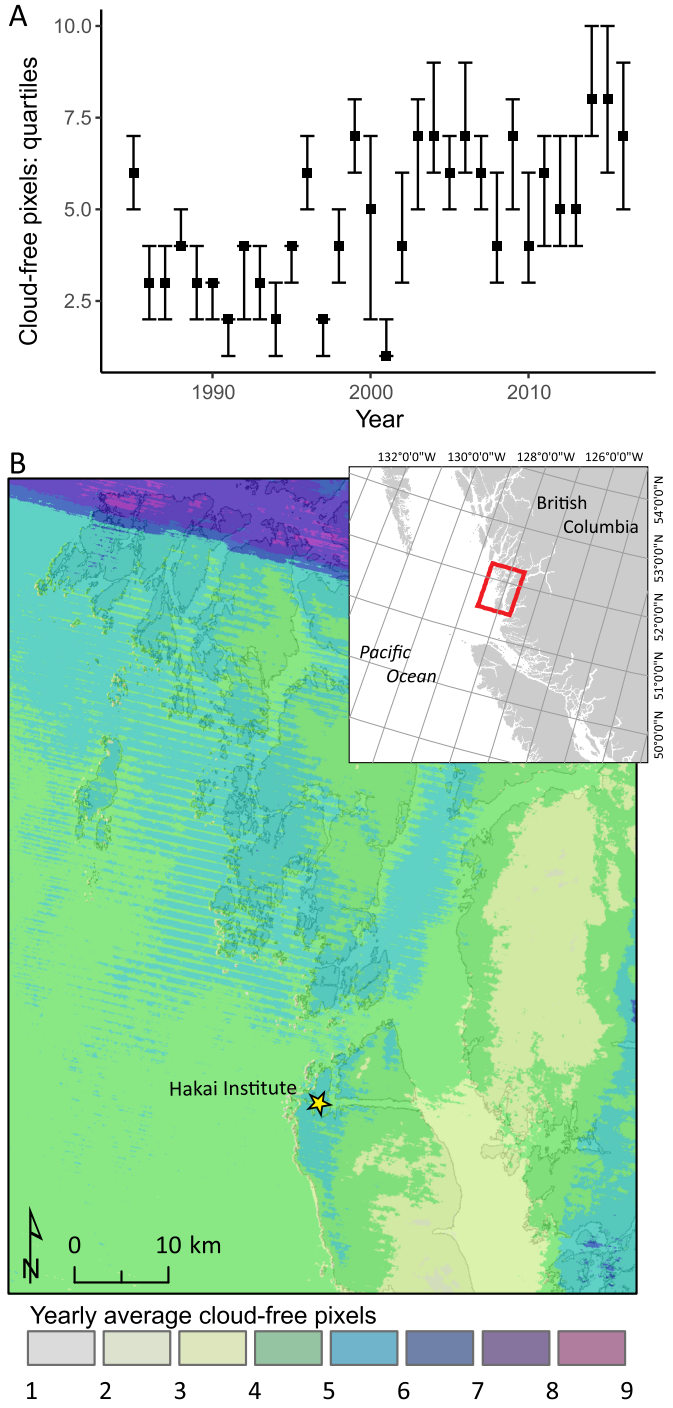

Fig. 3. A. Number of valid pixels available between June and September from all Landsat satellites per year between 1985 and 2016. B. Map of yearly average of valid pixels between June and September in the study area (over 32 years). Variability in valid pixel density is due to regions of overlapping Landsat tiles and cloud prevalence. Mean yearly cloud free pixels for the study area is 4.8.

(Table 2), with both classifications achieving > 80% overall accuracy. User's accuracy of kelp was 95% and 98% for Landsat and WorldView-2, respectively. Producer's accuracy of kelp using Landsat showed poor performance (56%) compared to WorldView-2 (72%). User's and producer's accuracies for water and kelp were not balanced because we used a stratified sampling strategy to reduce the importance of water on overall accuracy. Water is between 10 and 15 times more prevalent than kelp in the study area, even when considering potential habitat or nearshore waters only. The Landsat classification excluded areas within

Table 2
Confusion matrices for WorldView-2 (top) and Landsat (bottom) from field data. The Landsat matrix accuracies excludes the near shore masked area (30 m from land) from the calculations but present separate producer's and overall accuracy with those points included as being mislabelled as a reference. OA = overall accuracy, PA = producer's accuracy, UA = user's accuracy.

WorldView-2	Field reference			
	Water	Kelp		UA
Water	98	37		0.73
Kelp	2	97		0.98
PA	0.98	0.72		
			OA	**0.83**
				***n* = 234**

Landsat	Field reference				
	Water	Kelp	Masked	UA	
Water	96	32	*0*	0.75	
Kelp	2	41	*0*	0.95	
Masked	*2*	*61*	*0*		
PA mask excluded	0.98	0.56			
PA mask included	*0.96*	*0.31*			
OA mask excluded				**0.80**	***n* = 171**
OA mask included				*0.59*	*n = 234*

30 m from the shoreline and thus had a much lower overall accuracy when those areas are included (59% overall accuracy vs 80% when those areas are excluded). The confusion matrices (Table 2) show that both of the methods produce acceptable results for the study region when evaluated at single point locations. Differences in spatial distribution and resolution of the products are not reflected in these numbers but may have considerable implications in actual use cases.

3.2. Spatial resolution effects on detected kelp extent

Due to its higher spatial resolution (2 m), WorldView-2 has a more detailed detection of kelp canopies and patch configuration and detects kelp beds closer to shore in comparison to Landsat (30 m) (e.g. Fig. 4). Our results demonstrate that Landsat consistently overestimated the total area of canopy-forming kelp (Table 3). Overestimation was not present for the McMullin group, but > 60% for the Goose and Spider/Cultus regions.

Kelp patch size was found to influence the detectability of kelp at different sensor spatial resolutions. Fig. 5A shows the proportion of kelp extent derived from 2 m WorldView-2 imagery to the extent derived from WorldView-2 imagery resampled at 30 m (the resolution of Landsat imagery) summarized for each image region. The McMullin region, which has large offshore kelp beds, showed a better agreement with the resampled 30 m kelp extent. In the Spider-Cultus region, where beds are fringing and much smaller in extent, there was lowest proportion of overlap 2 m and 30 m derived kelp extents. Fig. 5B shows the relationship between detected kelp patch extent for a 2 m pixel and a 30 m pixel for the different regions as a function of the minimal detection cut-off at 30 m. The area trajectories are quite different between island groups with the slope being related to the average patch density as can be seen in Fig. 5A. The trajectories converge between a cut-off of 20–30% which corresponds to a consistent overestimation of the kelp area of near 50%. The Landsat derived kelp extents are in a similar range (Table 3), and thus relatively insensitive to patch density and configuration with the exception of the Spider-Cultus group where most kelp occurred in small beds fringing the shoreline.

Percent of surface kelp extent within 30 m from shore ranged from 28 to 75% (average 43%) across all regions (Table 3). The Goose and McMullin regions had the largest areas of offshore kelp with > 60% of the kelp present in these regions occurring further than 30 m offshore. Conversely, the Admiral-Tribal and Spider-Cultus regions had the

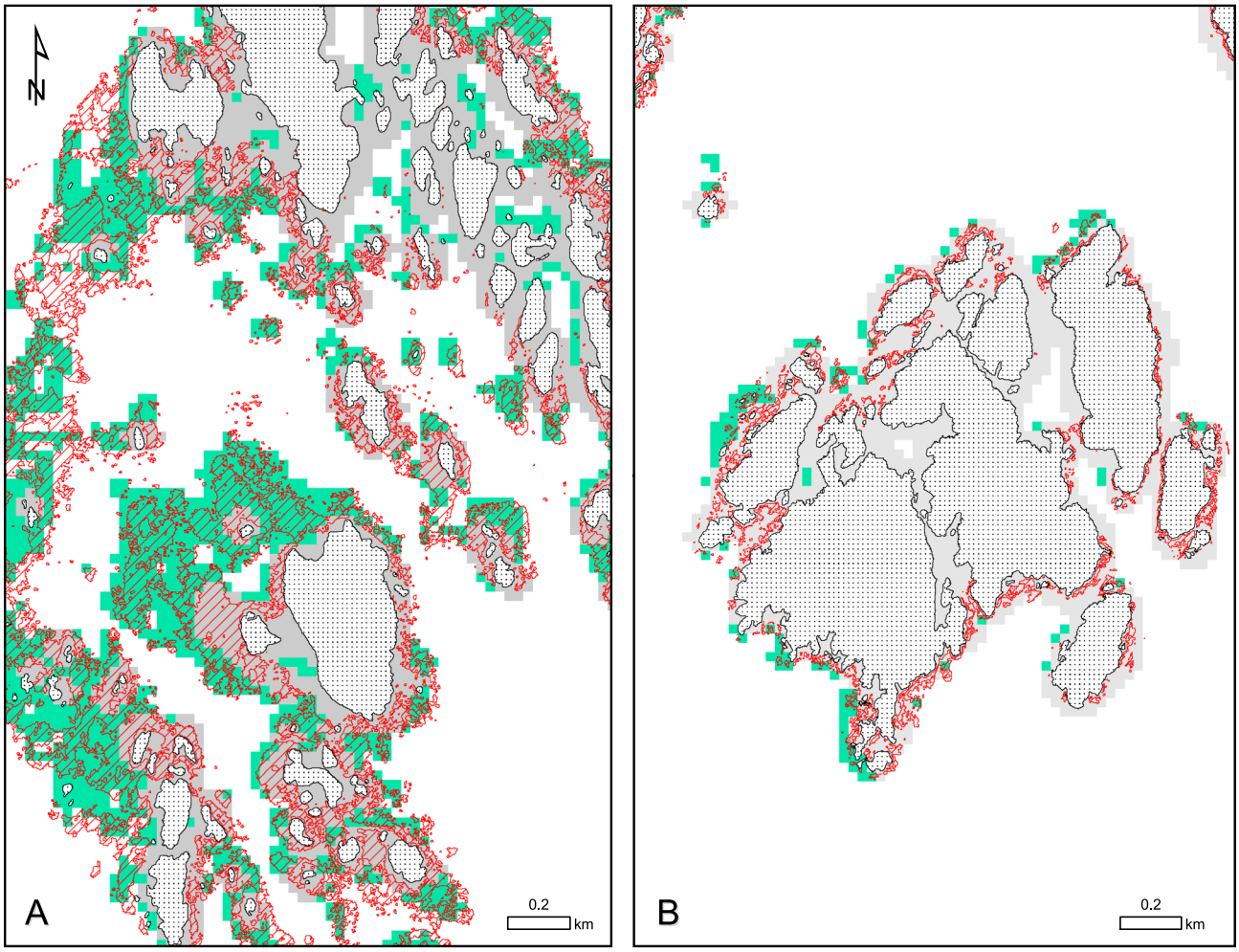

Fig. 4. Subsets of kelp classified from Landsat (green) and WorldView-2 imagery (red striated) for the McMullin Group (A) and the Admiral Group (B). Stippled region indicates land while shaded region indicates the land and 30 m buffer derived from Landsat imagery. (For interpretation of the references to colour in this figure legend, the reader is referred to the web version of this article.)

Table 3
Detected kelp extent for WorldView-2 and Landsat.

Island group	Landsat kelp extent [ha]	WorldView-2 kelp extent [ha]	Relative Landsat kelp area to WorldView-2 [%] (WV2 = 100%)	Proportion kelp (WorldView-2) under landmask (30 m from shore) [%]
Stryker|Athlone	185.0	165.6	111.7%	46.6%
McMullin	168.3	172.6	97.5%	28.0%
Tribal|Admiral	96.6	85.4	113.1%	72.7%
Goose	370.6	231.1	160.3%	30.6%
Simmonds	54.7	44.1	124.1%	53.8%
Spider|Cultus	165.1	47.3	349.1%	75.0%
Sterling|Calvert	139.4	114.6	121.6%	46.9%
All groups	1179.7	860.6	137.0%	43.1%

majority of kelp (> 70%) present within 30 m of shore. These areas are masked in the Landsat analyses and thus result not included in the kelp detection.

3.3. Tide sensitivity

Kelp fronds and stipes are attached to the seafloor and float up to the surface aided by gas-filled bladders to promote light exposure of the blade surface. The proportion of the kelp fronds and blades present at or directly near the water surface depend strongly on water currents and tide stage (Britton-Simmons et al., 2008). We evaluated the differences in detection for both satellites for images with 2.1 m difference in tide stage (Table 1). For WorldView-2, the extent for surface kelp detected at low tide (0.6 m) was 42% greater than compared to high tide (2.5 m). For Landsat 8, the surface extent of low tide kelp (1.5 m) was 41% greater than high tide (3.6 m) (Table 4). While taken at different tide stages, the results are similar in size and quite large both in absolute area as well as measured as proportion of the detected kelp extent. Note that the exact area is a rather small subset of the study area based on image availability. We included these results to emphasize the consequences of a large tidal regime on kelp detection. The kelp mapping tool we present in this paper is intended to overcome the issue of single scene classification by analyzing multiple image pixels and therefore improving the likelihood of capturing lower tide levels, and therefore peak surface extent and biomass conditions.

3.4. Kelp trends 1985–2006

Comparison of kelp extent for the study area over the three decades since 1985 revealed an increase in kelp extent for almost all areas (Table 5). A larger increase in kelp extent is observed from 1985 to 2006 than 2007–2016 where kelp in the Tribal-Admiral and Simmonds regions showed a decreased extent. The comparison of the three separate decades to the accumulated kelp extent over the entire period

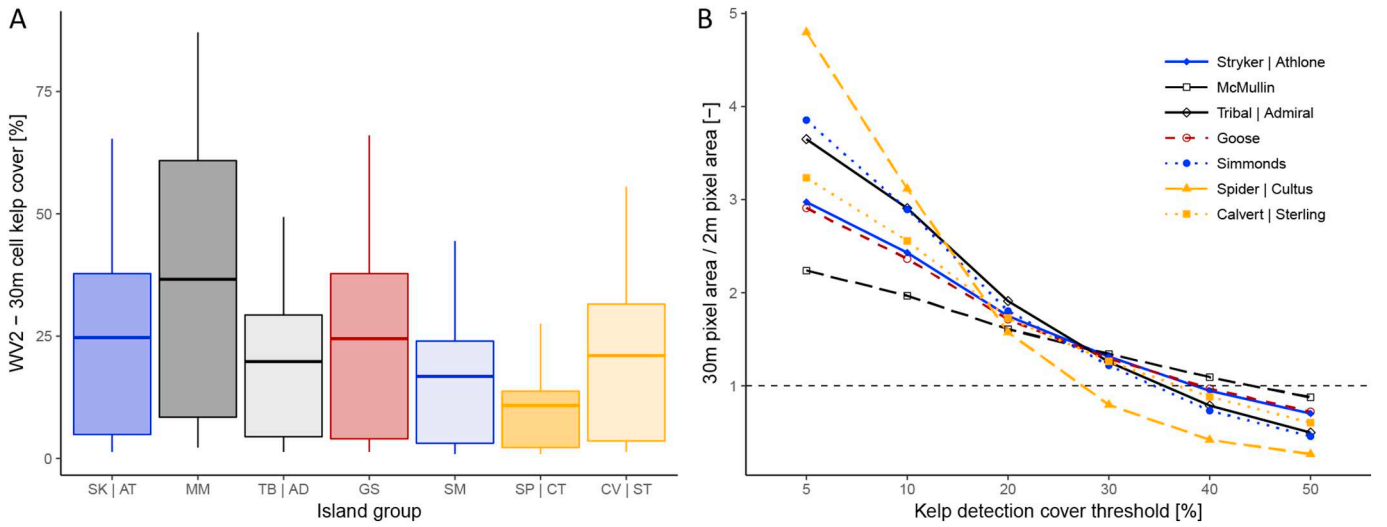

Fig. 5. A: Mean kelp cover in WorldView-2 imagery resampled to a 30 m cell size for each image region. B: Area of kelp at 30 m cell size as derived from 2 m WorldView 2 data as a function of cover percentage threshold to be considered kelp. CV|ST = Calvert|Stirling, GS = Goose, MM = McMullin, SM = Simonds, SP|CT = Spider|Cultus, SK|AT = Stryker|Athlone, TB|AD = Tribal|Admiral.

Table 4
Comparison of kelp extent classification using Landsat 8 and WorldView-2 imagery at different tidal states.

Sensor	Low tide kelp extent (ha)	High tide kelp extent (ha)	Difference (ha)	Difference (%)
WorldView-2	13.90	8.10	5.80	42
Landsat 8	20.19	11.93	8.26	41

demonstrated that kelp extent within the overall study region is variable at decadal time scales, with the extent over the entire period being more than twice the size of the extent of the single decade with the most cover.

4. Discussion

The availability of the entire Landsat archive of imagery through Google Earth Engine provides unprecedented opportunities to create seamless products of land cover to examine current and past patterns of ecologically important habitats. The 30 m pixel size is ideally suited for terrestrial land cover, forestry and habitat applications (Kerr and Ostrovsky, 2003), but also has great potential for mapping near-shore environments (Traganos et al., 2018). Kelp forests, composed of bull kelp (*N. luetkeana*) and giant kelp (*M. pyrifera*), are one such habitat that is very important to the ecological, cultural and economic integrity of coastal British Columbia. Landsat images, and other moderate resolution sensors, have been successfully applied in mapping large kelp forests in the Santa Barbara Channel, California (Cavanaugh et al., 2010, 2011), but the convoluted shorelines, small beds, and fringing beds that characterize kelp distribution on much of the coastline of British Columbia presents a unique challenge for applying Landsat imagery to map kelp in this region. Furthermore, a larger tidal region and higher frequency of cloud cover reduce the availability of usable imagery for this region. In this paper we created a tool within Google Earth Engine to overcome these issues for mapping kelp extent which takes advantage of all available imagery and provides analytical efficiency by removing the requirement of downloading individual image scenes. We compared outputs from the Google Earth Engine kelp mapping tool with paired WorldView-2 high resolution satellite imagery and field data to understand the capabilities and limitations of mapping kelp using Landsat imagery for the Central Coast of British Columbia.

Table 5
Kelp extent (hectares) derived using Google Earth Engine kelp mapping tool for each image region for three time periods.

Island group	Kelp extent (ha) 1985–1996	Kelp extent (ha) 1997–2006	Kelp extent (ha) 2007–2016	Kelp extent (ha) 1985–2016
Stryker|Athlone	65.5	86.0	**95.9**	**185.0**
McMullin	48.5	73.8	**89.2**	**168.3**
Tribal|Admiral	28.0	**47.0**	36.0	**96.6**
Goose	109.6	168.4	**177.8**	**370.6**
Simmonds	19.1	**31.1**	27.1	**54.7**
Spyder|Cultus	51.0	62.7	**67.1**	**165.1**
Sterling|Calvert	47.6	56.4	**76.1**	**139.4**
All Groups	**369.4**	**525.5**	**569.2**	**1179.7**

The overarching goal of the Google Earth Engine kelp mapping tool is to generate consistent and reliable outputs of kelp extent at a regional scale (10 s–100 s km^2). Early attempts determined Landsat is unable to detect kelp present close to shore and therefore a 30 m buffer was applied to avoid classifying pixels with any land or terrestrial vegetation as kelp. From the WorldView-2 classification, we determined that between 28% and 75% of kelp canopies are present in this shore fringe (Table 3, Fig. 4). When considering the entire study region, 43% of kelp detected by WorldView-2 was present within this nearshore zone masked from the Landsat product. While this is a serious limitation of any products derived at the 30 m Landsat resolution, the regions in our study area with most kelp in the shore fringe have much less kelp in general. Therefore, detected trends in kelp cover for the high resolution WorldView-2 products and the Landsat derived maps still correspond well. When comparing the accuracy of Landsat 8 imagery and WorldView-2 to field plots, the accuracy of kelp detection with Landsat is very close the accuracy of WorldView-2 when the masked nearshore zone was not considered (Table 2). Although the methods for mapping kelp extent using Landsat imagery miss a portion of kelp, particularly in fringing beds near the coastline, detections are reliable in areas where the Landsat imagery does detect kelp as indicated by the high user's accuracy. The lower values of producer's accuracy indicate that considerable areas of kelp are missed in the Landsat classification in each year of detection. The omission can be partially countered by accumulating several years of kelp data rather than analyzing individual years, but we expect that certain areas with sparse kelp cover at the water surface will be missed consistently.

In this study we evaluated kelp extent as presence-absence on a pixel-by-pixel basis. The result of this procedure is an overestimation of kelp area from Landsat imagery because the entirety of each Landsat pixels is counted as kelp even when the pixel only has partial kelp cover. The lower cut-off for marking a partially covered pixel as kelp is mainly dictated by our detection ability while avoiding false positives, but a higher cut-off could be adopted to reduce the effect pixel size on estimated kelp area. The degree of overestimation is dependent on patch configuration, canopy density, and the minimum cover detected as kelp (Fig. 5). Trends in the scale effect converge between 20 and 30% cutoff, which results in a 1.5 times overestimation of kelp area. Overestimation in our results as compared to Worldview-2 are on average around this sweet spot with 1.37 times overestimation (Table 3), but still show considerable differences between groups. McMullin groups have many large and continuous kelp beds and a slight underestimations while overestimation groups with more sparse kelp beds is larger. The current detection process falls roughly in this detection limit leading to a fairly constant rate of overestimation between most island groups (Table 3). While little potential is available for detection in the shore fringe, partial kelp cover or canopy density may be estimated from the spectral response in each pixel. The estimation of kelp cover would need reliable concurrent observations with image acquisition, which is challenging because of the temporal accumulation of observations in the current Landsat process. However, annual time series of kelp cover are currently being collected using unmanned aerial systems (UAS) imaging for select parts of the study area, providing suitable calibration data for future analyses.

The novel process to derive kelp extent from Landsat images we present in this paper relied heavily on temporal compositing of all available images within the Google Earth Engine image archive (Fig. 2). The accumulation of observations throughout the growing season and years eliminates the requirement to manually find and select good images for the detection process. In the nearshore environment, the ideal image is increasingly difficult to define because suitability depends on many factors including cloud cover, wave conditions, sun glint, tide stage, and kelp phenology. Many of these factors change quickly and asynchronously throughout images and geographically along the coast. In our current analysis of changes in kelp cover, we analysed products at the decadal time scale to allow for sufficient data to accumulate and achieve stable results. In the near future, we anticipate generating kelp extent products at shorter temporal intervals because of the increased image acquisition frequencies with modern satellite imagery (e.g. Sentinel-2) available within the Google Earth Engine image library. The advent of newer sensors with better spatial resolution should improve outputs and faster satellite revisit times or integrating multiple sensor platforms should allow for the creation of reliable annual kelp extents.

When comparing kelp cover across decades, we saw an increase in kelp extent for almost all areas, with much of the increase occurring between 1990 and 2000 (Table 5). Overall, these results are consistent with increases in kelp abundances reported for this region (North American Pacific Fjordland) by Krumhansl et al. (2016). Reports from kelp inventory surveys conducted for the region analysed differences in kelp extent and biomass for part of the study area between 1993 and 2007 using aerial photo interpretation (Sutherland et al., 2008). Between those time periods, there was an observed increase in *M. pyrifera* cover in the majority of the study area, which is consistent with the results from this study. However, in many areas the extent of *N. luetkeana* declined leading to a slight overall decline of kelp cover. *N. luetkeana* occurs in rather sparse beds compared to *M. pyrifera*. Sutherland et al. (2008) marks *N. luetkeana* beds > 15% surface cover as high density, for *M. pyrifera* this was > 40%. Under these conditions it is less likely that these lower density *N. luetkeana* beds would be detected by Landsat imagery. The shift in species can also explain part of the variability in kelp locations we observe; the total area with kelp cover over the entire study period is nearly twice the size of the largest individual decadal extent.

There are many factors that may be driving kelp dynamics in the study region. These include oceanographic patterns (e.g. Pacific Decadal Oscillation, El Nino Southern Oscillation, North Pacific Gyre Oscillation), ecological factors (e.g. sea otters, urchin grazing), and ocean condition (e.g. sea surface temperature, storms). Other studies that have examined drivers of kelp dynamics (Cavanaugh et al., 2011; Pfister et al., 2017; Young et al., 2015) rely on the availability of a long term datasets of kelp extent and biomass. The tool we present in this paper is intended as the start to the creation of such a dataset. Furthermore, the nature of the Google Earth Engine as a cloud computing tool means that the code developed for our study region can be adapted at a coast-wide scale in British Columbia and to other coastal regions globally to develop similar datasets.

5. Conclusions

Canopy-forming kelp species are ecologically important species but current and comprehensive inventories for these species are lacking for most of the 25,000 km of Canada's Pacific coast. In this paper we introduced a novel method to rapidly assess and detect canopy-forming kelp extent from the Landsat image archive within Google Earth Engine. While Landsat has limitations for detecting very sparse and shore fringing kelp canopies, the process we developed produced results that are consistent with higher resolution product and field data when comparing the same regions. By accumulating data over multiple years and from many scenes, we were able to avoid effects of seasonal and annual variability in detected area introduced by tidal differences. The identification of increasing trends in kelp cover over the last 3 decades indicates a promising method for assessing the status and ecological dynamics of kelp ecosystems in this region. The methods are a solid basis for further refinement and application to other regions both within British Columbia and elsewhere. Future developments may include integrating newer sensors (e.g. Sentinel 2) in Google Earth Engine.

Acknowledgements

This work was funded supported by the Hakai Institute (www.hakai.org), Fisheries and Oceans Canada's National Marine Conservation Targets Program and the Strategic Program for Ecosystem Research and Analysis, and the University of Victoria, Canada. A portion of the WorldView-2 imagery was provided by the DigitalGlobe Foundation.

References

Banskota, A., Kayastha, N., Falkowski, M.J., Wulder, M.A., Froese, R.E., White, J.C., 2014. Forest monitoring using landsat time series data: a review. Can. J. Remote. Sens. 40, 362–384. https://doi.org/10.1080/07038992.2014.987376.

Bell, T.W., Cavanaugh, K.C., Reed, D.C., Siegel, D.A., 2015a. Geographical Variability in the Controls of Giant Kelp Biomass Dynamics 2010–2021. https://doi.org/10.1111/jbi.12550.

Bell, T.W., Cavanaugh, K.C., Siegel, D.A., 2015b. Remote monitoring of giant kelp biomass and physiological condition: an evaluation of the potential for the hyperspectral infrared imager (HyspIRI) mission. Remote Sens. Environ. https://doi.org/10.1016/j.rse.2015.05.003.

Botha, E.J., Brando, V.E., Anstee, J.M., Dekker, A.G., Sagar, S., 2013. Increased spectral resolution enhances coral detection under varying water conditions. Remote Sens. Environ. 131, 247–261. https://doi.org/10.1016/j.rse.2012.12.021.

Britton-Simmons, K., Eckman, J.E., Duggins, D.O., 2008. Effect of tidal currents and tidal stage on estimates of bed size in the kelp *Nereocystis luetkeana*. Mar. Ecol. Prog. Ser. 355, 95–105. https://doi.org/10.3354/meps07209.

Canada – British Columbia Marine Protected Area Network Strategy, 2014. https://www.for.gov.bc.ca/tasb/slrp/pdf/ENG_BC_MPA_LOWRES.pdf, Accessed date: 21 April 2018.

Cavanaugh, K., Siegel, D., Kinlan, B., Reed, D., 2010. Scaling giant kelp field measurements to regional scales using satellite observations. Mar. Ecol. Prog. Ser. 403, 13–27. https://doi.org/10.3354/meps08467.

Cavanaugh, K., Siegel, D., Reed, D., Dennison, P., 2011. Environmental controls of giant-kelp biomass in the Santa Barbara Channel, California. Mar. Ecol. Prog. Ser. 429, 1–17. https://doi.org/10.3354/meps09141.

Clark, D.K., Gordon, H.R., Voss, K.J., Ge, Y., Broenkow, W., Trees, C., 1997. Validation of atmospheric correction over the oceans. J. Geophys. Res. 102, 17209–17217. https://

doi.org/10.1029/96JD03345.
Clasen, J.L., Shurin, J.B., 2015. Kelp forest size alters microbial community structure and function on Vancouver Island, Canada. Ecology 96, 862–872. https://doi.org/10.1890/13-2147.1.sm.
Cohen, W.B., Goward, S.N., 2004. Landsat's Role in Ecological Applications of Remote Sensing. 54. pp. 535–545.
Crawford, W.R., Huggett, W.S., Woodward, M.J., Daniel, P.E., 1985. Summer circulation of the waters in Queen Charlotte sound. Atmosphere-Ocean 23, 393–413. https://doi.org/10.1080/07055900.1985.9649235.
Dayton, P.K., 1985. Ecology of kelp communities. Annu. Rev. Ecol. Syst. 16, 215–245. https://doi.org/10.1146/annurev.es.16.110185.001243.
Dean, T.A., Schroeter, S.C., Dixon, J.D., 1984. Effects of grazing by two species of sea urchins (*Strongylocentrotus franciscanus* and *Lytechinus anamesus*) on recruitment and survival of two species of kelp (*Macrocystis pyrifera* and *Pterygophora californica*). Mar. Biol. 78, 301–313. https://doi.org/10.1007/BF00393016.
DFO, 2017. A framework for identification of ecological conservation priorities for marine protected area network design and its application in the Northern Shelf bioregion. In: DFO Canadian Science Advisory Secretariat Science Advice Report 2017/019.
DFO, 2018. Reassessment of the ecologically and biologically significant areas (EBSAs) in the Pacific Northern Shelf. In: DFO Canadian Science Advisory Secretariat Science Advice Report 2018/040.
DigitalGlobe, 2016. WorldView-2 data sheet. https://dg-cms-uploads-production.s3.amazonaws.com/uploads/document/file/98/WorldView2-DS-WV2-rev2.pdf.
Duarte, C.M., Cebrian, J., 1996. The fate of mangrove autotrophic production. Limnol. Oceanogr. 41, 1758–1766.
El-Askary, H., Abd El-Mawla, S.H., Li, J., El-Hattab, M.M., El-Raey, M., 2014. Change detection of coral reef habitat using Landsat-5 TM, Landsat 7 ETM+ and Landsat 8 OLI data in the Red Sea (Hurghada, Egypt). Int. J. Remote Sens. 35 (6), 2327–2346.
Estes, J.A., Duggins, D.O., 2010. Sea otters and kelp forests in Alaska: generality and variation in a community ecological paradigm. Ecol. Soc. Am. 65, 75–100.
Estes, J.A., Palmisano, J.F., 1974. Sea otters: their role in structuring nearshore communities. Science 185, 1058–1060. https://doi.org/10.1126/science.185.4156.1058. 80-.
Field, E.J., 1996. Kelp Inventory, 1993, Areas of the British Columbia Central Coast from Hakai Passage to the Bardswell Group.
Foreman, M.G.G., Pal, B., Merryfield, W.J., 2011. Trends in upwelling and downwelling winds along the British Columbia shelf. J. Geophys. Res. Ocean. 116, 1–11. https://doi.org/10.1029/2011JC006995.
Gerace, A.D., Schott, J.R., 2012. Over-water Atmospheric Correction for Landsat's New OLI Sensor. 8372. pp. 837211. https://doi.org/10.1117/12.919304.
Gorelick, N., Hancher, M., Dixon, M., Ilyushchenko, S., Thau, D., Moore, R., 2017. Google earth engine: planetary-scale geospatial analysis for everyone. Remote Sens. Environ. 202, 18–27. https://doi.org/10.1016/j.rse.2017.06.031.
Government of Canada, 2011. National Framework for Canada's Network of Marine Protected Areas. Fisheries and Oceans Canada, Ottawa (31 pp).
Hannah, L., St. Germain, C., Jeffery, S., Patton, S.O.M., 2017. Application of a framework to assess vulnerability of biological components to ship-source oil spills in the marine environment in the Pacific Region. In: DFO Canadian Science Advisory Secretariat Research Document. 2017/057, (ix+145p).
Harrold, C., Light, K., Lisin, S., 1998. Organic enrichment of submarine-canyon and continental-shelf benthic communities by macroalgal drift imported from nearshore kelp forests. Limnol. Oceanogr. 43, 669–678. https://doi.org/10.4319/lo.1998.43.4.0669.
Hedley, J.D., Harborne, A.R., Mumby, P.J., 2005. Simple and robust removal of sun glint for mapping shallow-water benthos. Int. J. Remote Sens. 26 (10), 2107–2112.
Hossain, M.S., Bujang, J.S., Zakaria, M.H., Hashim, M., 2016. Marine and human habitat mapping for the coral triangle initiative region of Sabah using Landsat and Google earth imagery. Mar. Policy 72, 176–191.
Hu, C., 2009. A novel ocean color index to detect floating algae in the global oceans. Remote Sens. Environ. 113, 2118–2129. https://doi.org/10.1016/j.rse.2009.05.012.
Hu, C., Muller-Karger, F.E., Andrefouet, S., Carder, K.L., 2001. Atmospheric correction and cross-calibration of Landsat-7/ETM+ imagery over aquatic environments: a multiplatform approach using SeaWiFS/MODIS. Remote Sens. Environ. 78, 99–107. https://doi.org/10.1016/S0034-4257(01)00252-8.
Jackson, J.M., Thomson, R.E., Brown, L.N., Willis, P.G., Borstad, G.A., 2015. Satellite chlorophyll off the British Columbia coast. J. Geophys. Res. 120, 4709–4728.
Kay, S., Hedley, J.D., Lavender, S., 2009. Sun glint correction of high and low spatial resolution images of aquatic scenes: a review of methods for visible and near-infrared wavelengths. Remote Sens. 1 (4), 697–730.
Kerr, J., Ostrovsky, M., 2003. From space to species: ecological applications for remote sensing. Trends Ecol. Evol. 18, 299–305. https://doi.org/10.1016/S0169-5347(03)00071-5.
Krumhansl, K.A., Scheibling, R.E., 2012. Production and fate of kelp detritus. Mar. Ecol. Prog. Ser. 467, 281–302. https://doi.org/10.3354/meps09940.
Krumhansl, K.A., Okamoto, D.K., Rassweiler, A., Novak, M., Bolton, J.J., Cavanaugh, K.C., Wernberg, T., Anderson, R.J., Barrett, N.S., Buschmann, A.H., Carr, M.H., Watson, J., Witman, J.D., Byrnes, J.E.K., 2016. Global patterns of kelp forest change over the past half-century. PNAS 1–6. https://doi.org/10.1073/pnas.1606102113.
Lastra, M., Page, H.M., Dugan, J.E., Hubbard, D.M., Rodil, I.F., 2008. Processing of allochthonous macrophyte subsidies by sandy beach consumers: estimates of feeding rates and impacts on food resources. Mar. Biol. 154, 163–174. https://doi.org/10.1007/s00227-008-0913-3.
Lin, S.P., Novitski, L.N., Qi, J.G., Stevenson, R.J., Landsat, T.M., 2018. ETM+ and machine-learning algorithms for limnological studies and algal bloom management of inland lakes. J. Appl. Remote. Sens. 12 (2).
Mao, Z., Pan, D., He, X., Chen, J., Tao, B., Chen, P., Hao, Z., Bai, Y., Zhu, Q., Huang, H., 2016. A unified algorithm for the atmospheric correction of satellite remote sensing data over land and ocean. Remote Sens. 8. https://doi.org/10.3390/rs8070536.
Markel, R., Shurin, J., 2015. Indirect effects of sea otters on rockfish (*Sebastes* spp.) in giant kelp forests. Ecology 96, 2877–2890 (doi:10.1890).
Marzinelli, E.M., Williams, S.B., Babcock, R.C., Barrett, N.S., Johnson, C.R., Jordan, A., Kendrick, G.A., Pizarro, O.R., Smale, D.A., Steinberg, P.D., 2015. Large-scale geographic variation in distribution and abundance of Australian deep-water kelp forests. PLoS One 10, 1–21. https://doi.org/10.1371/journal.pone.0118390.
McLaren, D., Rahemtulla, F., Gitla, Fedje, D., 2015. Archaeological evidence for long-term occupation of the central coast of British Columbia. In: B.C. Stud, pp. 155–191.
Murray, N.J., Keith, D.A., Simpson, D., Wilshire, J.H., Lucas, R.M., 2018. Remap: an online remote sensing application for land cover classification and monitoring. Methods Ecol. Evol. 9 (9), 2019–2027.
Nichol, L.M., Watson, J.C., Abernethy, R., Rechsteiner, E., Towers, J., 2015. Trends in the abundance and distribution of sea otters (*Enhydra lutris*) in British Columbia updated with 2013 survey results. In: DFO Can. Sci. Advis. Secr. Res. Doc. 3848, https://doi.org/10.13140/RG.2.1.2515.2886. (vii + 44 pp).
Orr, M., Zimmer, M., Jelinski, D.E., Mews, M., 2008. Wrack deposition on different beach types: spatial and temporal variation in the pattern of subsidy. Ecol. Soc. Am. 86, 1496–1507.
Pekel, J.-F., Cottam, A., Gorelick, N., Belward, A.S., 2016. High-resolution mapping of global surface water and its long-term changes. Nature 540, 418–422. https://doi.org/10.1038/nature20584.
Pfister, C.A., Berry, H.D., Mumford, T., 2017. The dynamics of kelp forests in the northeast Pacific Ocean and the relationship with environmental drivers. J. Ecol. 1–14. https://doi.org/10.1111/1365-2745.12908.
Polis, G.A., Hurd, S.D., 1996. Linking marine and terrestrial food webs: allochthonous input from the ocean supports high secondary productivity on small islands and coastal land communities. Am. Nat. 147, 396–423.
Raffaelli, D., Hawkins, S.J., 1996. Intertidal Ecology. Chapman & Hall, London.
Richter, R., Schlapfer, D., 2012. Atmospheric/topographic correction for airborne imagery: ATCOR-4 User Guide. DLR IB 565-02.
Ritchie, J.C.J., Zimba, P.P.V., Everitt, J.H.J., 2003. Remote sensing techniques to assess water quality. Photogramm. Eng. Remote. Sens. 69, 695–704. https://doi.org/10.14358/PERS.69.6.695.
Shaffer, J.A., 2000. The Strait of Juan de Fuca. J. Coast. Res. 16, 768–775.
Stehman, S.V., Czaplewski, R.L., 1998. Design and analysis for thematic map accuracy assessment: fundamental principles. Science 344, 331–344 80-.
Steneck, R.S., Graham, M.H., Bourque, B.J., Corbett, D., Erlandson, J.M., Estes, J.A., Tegner, M.J., 2002. Kelp forest ecosystems: biodiversity, stability, resilience and future. Environ. Conserv. 29, 436–459. https://doi.org/10.1017/S0376892902000322.
Sutherland, I., Karpouzi, V., Mamoser, M., Carswell, B., 2008. Kelp Inventory, 2007: Areas of the British Columbia Central Coast from Hakai Passage to the Bardswell Group.
Thomson, R.E., 1981. Oceanography of the British Columbia Coast. (Ottawa).
Torres-Pulliza, D., Wilson, J.R., Darmawan, A., Campbell, S.J., Andréfouët, S., 2013. Ecoregional scale seagrass mapping: a tool to support resilient MPA network design in the Coral Triangle. Ocean Coast. Manag. 80, 55–64.
Traganos, D., Aggarwal, B., Poursanidis, D., Topouzelis, K., Chrysoulakis, N., Reinartz, P., 2018. Towards global-scale seagrass mapping and monitoring using Sentinel-2 on Google earth engine: the case study of the Aegean and Ionian seas. Remote Sens. 10 (8).
Watson, J., Estes, J.A., 2011. Stability, resilience, and phase shifts in rocky subtidal communities along the west coast of Vancouver Island, Canada published by: Ecological Society of America Stable URL: http://www.jstor.org/stable/23047556 your use of the JSTOR archive indicate. Ecol. Monogr. 81, 215–239. https://doi.org/10.1890/10-0262.1.
Wilmers, C.C., Estes, J.A., Edwards, M., Laidre, K.L., Konar, B., 2012. Do trophic cascades affect the storage and flux of atmospheric carbon? An analysis of sea otters and kelp forests. Front. Ecol. Environ. 10, 409–415. https://doi.org/10.1890/110176.
Young, M.A., Cavanaugh, K.C., Bell, T.W., Raimondi, P.T., Edwards, C.A., Drake, P.T., Erikson, L., Storlazzi, C., 2015. Environmental controls on spatial patterns in the long-term persistence of giant kelp in central California. Ecology 86, 150823154921001. https://doi.org/10.1890/15-0267.1.
Zhu, Z., Wang, S., Woodcock, C.E., 2015. Improvement and expansion of the Fmask algorithm: cloud, cloud shadow, and snow detection for Landsats 4-7, 8, and Sentinel 2 images. Remote Sens. Environ. 159, 269–277. https://doi.org/10.1016/j.rse.2014.12.014.
Zurqani, H.A., Post, C.J., Mikhailova, E.A., Schlautman, M.A., Sharp, J.L., 2018. Geospatial analysis of land use change in the Savannah river basin using Google earth engine. Int. J. Appl. Earth Obs. Geoinf. 69, 175–185.